2010

Bent-Core Liquid Crystal Elastomers

Rafael Verduzco
Paul Luchette
Seung Ho Hong
John Harden
Elaine DiMasi, et al.

Bent-core liquid crystal elastomers

Rafael Verduzco,†*[a] Paul Luchette,[b] Seung Ho Hong,[c] John Harden,[b] Elaine DiMasi,[d] Peter Palffy-Muhoray,[b] S. Michael Kilbey II,[ae] Samuel Sprunt,[c] Jim T. Gleeson[c] and Antal Jákli[b]

Received 16th June 2010, Accepted 28th July 2010
DOI: 10.1039/c0jm01920h

Liquid crystal (LC) elastomers with bent-core side-groups incorporate the properties of bent-core liquid crystals in a flexible and self-supporting polymer network. Bent-core liquid crystal elastomers (BCEs) with uniform alignment were prepared by attaching a reactive bent-core LC to poly(hydrogenmethylsiloxane) and crosslinking with a divinyl crosslinker. Phase behavior studies indicate a nematic phase over a wide temperature range that approaches room temperature, and thermoelastic measurements show that these BCEs can reversibly change their length by more than a factor of two upon heating and cooling. Small-angle X-ray scattering studies reveal multiple, broad low-angle peaks consistent with short-range smectic C order of the bent-core side groups. A comparison of these patterns with predictions of a Landau model for short-range smectic C order shows that the length scale for smectic ordering in BCEs is similar to that seen in pure bent-core LCs. The combination of rubber elasticity and smectic ordering of the bent-core side groups suggests that BCEs may be promising materials for sensing, actuating, and other advanced applications.

Introduction

Liquid crystal elastomers (LCEs) bring together the elasticity and flexibility of a rubber with the optical properties and responsiveness of liquid crystals (LCs). Due to the coupling of orientational order and mechanical strain, LCEs exhibit remarkable behavior not observed in either elastomers or LCs separately, such as changing shape reversibly in response to light,[1,2] temperature,[3] and electric fields.[4] Recent manuscripts[5,6] and a monograph[7] provide comprehensive reviews of LCEs.

The first LCE was made by attaching small-molecule LCs to a polymer network[8] composed of flexible polysiloxane chains (see schematic Fig. 1). Subsequent work has revealed that the chemical structure of the elastomeric network has a dramatic effect on the behavior of LCEs. For example, the incorporation of mesogens in the polymer backbone to make main-chain LCEs enhances the coupling between the LC order parameter and the strain of the polymer network, leading to greater temperature-induced shape changes.[3,5] The present work focuses on LCEs with bent-core side groups. Bent-core LCs exhibit a variety of potentially useful properties not typically seen in calamitic, or rod-like, nematics.[9] Most notably, bent-core LCs can form polar and chiral structures even though the molecules are achiral,[10] and bent-core molecules exhibit novel LC phases.[11] Bent-core LCs with a nematic phase are relatively rare, and recent studies of bent-core nematics have uncovered a number of unusual properties, including the presence of biaxiality,[12,13] huge flexoelectricity,[14] large flow-induced birefringence,[15] novel self-assembly behavior,[16,17] and short-range smectic-C ordering.[18–20]

The motivation for making bent-core LCEs (BCEs) is twofold. The spontaneous chirality and large flexoelectricity of bent-core LCs lead to potential applications, and a free-standing, elastomeric bent-core material can more easily be incorporated in a device. However, the consequences of coupling bent-core LCs with an elastomeric network have not been studied, and it is not clear whether or not a BCE will exhibit properties similar to those of bent-core LCs.

This paper addresses both the synthesis and structural properties of BCEs; flexoelectric measurements are the topic of a separate publication.[21] In the following, the preparation and structural characterization of BCEs are described for the first time. The preparation of BCEs takes advantage of the well-known Finkelmann method[22] for the synthesis of nematic LCEs using a reactive bent-core LC mesogen. The phase behavior and thermoelastic properties of the resulting aligned BCEs are fully characterized, and we compare the structural features of BCEs to bent-core liquid crystals.

Experimental

Materials

The starting materials ethyl 4′-hydroxybiphenyl-4-carboxylate, 4,6-dichloro resorcinol (**1**), 1-octanol, 1,4-bis(11-undeceneoxy)-benzene, 8-bromo-1-octene, tetrahydrofuran (anhydrous, ≥99.9%, inhibitor-free), benzene (*ReagentPlus*®, thiophene free, ≥99%), and triethylamine (ReagentPlus®, 99%) were purchased from Sigma-Aldrich and used as received. Thionyl chloride (Sigma-Aldrich, *ReagentPlus*®, 99.5%, low iron) was dried with

[a]*Center for Nanophase Materials Sciences, Oak Ridge National Laboratory, 1 Bethel Valley Road, Oak Ridge, TN, 37831, USA*
[b]*Chemical Physics Interdisciplinary Program and Liquid Crystal Institute, Kent State University, Kent, OH, USA. E-mail: mpalffy@cpip.kent.edu; Fax: +330-672-2959; Tel: +330- 672-2246*
[c]*Department of Physics, Kent State University, Kent, OH, 44242, USA. E-mail: ssprunt@kent.edu; Tel: +330-672-2682*
[d]*National Synchrotron Light Source, Brookhaven National Laboratory, Upton, NY, 11973, USA. E-mail: dimasi@bnl.gov*
[e]*Department of Chemistry, University of Tennessee, Knoxville, TN, 37966, USA. E-mail: mkilbey@ion.chem.utk.edu*
† Present address: Rice University, 6100 Main Street, MS-362, Houston, TX 77008. USA. E-mail: rafaelv@rice.edu Fax: 713-348-5478 Tel; 713-348-6492;

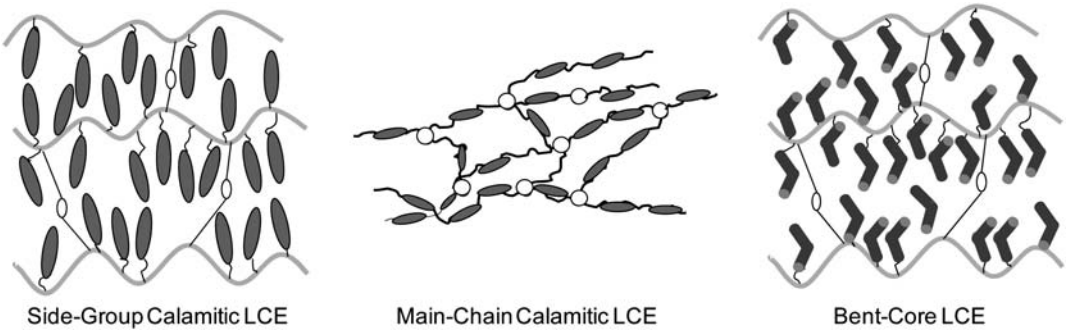

Fig. 1 Schematic of different types of LCEs. Side-chain calamitic LCEs are made by attaching a rod-like mesogen as a side-group to a polymer network. Main-chain LCEs incorporate the mesogen into the backbone of the polymer network. Side-group bent-core LCEs (BCEs) have bent-core mesogenic side groups attached to the polymer network *via* a flexible spacer.

calcium hydride, distilled at 85 °C, and stored under nitrogen. Ethyl acetate (ACS grade), hexanes (ACS grade), ethanol (ACS grade), and methanol (Baker Analyzed* Reagent, ACS Grade) were purchased from VWR and used as received. The bent-core liquid crystal without terminal vinyl groups was prepared as previously described.[23,24] All other reagents were purchased from Aldrich and used as received, unless otherwise noted.

4′-(8-Octyloxy)-1,1′-biphenyl-4-carbonyl chloride (2) and 4′-(8-octen-1-yloxy)-1,1′-biphenyl-4-carbonyl chloride (4)

Compounds (**2**) and (**4**) are precursors for the synthesis of reactive bent-core LC, and they were synthesized using methods analagous to those described by Fodor-Csorba *et al.*[23] The bent-core LC precursors (**2**) and (**4**) reported here have a shorter alkyl tail length but are otherwise identical to those reported by Fodor-Csorba *et al.* (**2**) **^{1}H NMR:** δ 0.8-0.9 (t, 3H, –CH_3), δ 1.20–1.40 (m, 8H, –CH_2–), δ 1.60–1.80 (m, 2H, –OCH$_2$CH$_2$CH_2–), δ 1.70–1.80 (m, 2H, –OCH$_2$CH_2–), δ 3.90–4.00 (t, 2H, –OCH_2–), δ 6.90–6.96 (d, 2H, aromatic H on biphenyl ortho to Ar–COC$_8$H$_{17}$), δ 7.50–7.56 (d, 2H, aromatic H on biphenyl meta to Ar–COC$_8$H$_{17}$), δ 7.60–7.66 (d, 2H, aromatic H on biphenyl meta to Ar–COCl), δ 8.06–8.12 (d, 2H, aromatic H on biphenyl ortho to Ar–COCl). (**4**) **^{1}H NMR:** δ 1.20–1.60 (m, 8H, –CH_2–), δ 1.60–1.80 (m, 2H, –OCH$_2$CH$_2$CH_2–), δ 1.90–2.10 (m, 2H, –OCH$_2$CH_2–), δ 3.90–4.00 (t, 2H, –OCH_2–), δ 4.86–4.98 (q, 2H, –CH=CH_2), δ 5.70–5.80 (m, 1H, –CH=CH$_2$), δ 6.90–6.96 (d, 2H, aromatic H on biphenyl ortho to Ar–COC$_8$H$_{17}$), δ 7.50–7.56 (d, 2H, aromatic H on biphenyl meta to Ar–COC$_8$H$_{17}$), δ 7.60–7.66 (d, 2H, aromatic H on biphenyl meta to Ar–COCl), δ 8.06–8.12 (d, 2H, aromatic H on biphenyl ortho to Ar–COCl).

4,6-Dichloro-1-hydroxy-3- [4′-(8-octyloxy)-1,1′-biphenyl-4-carboxylate]-phenylene (3). 4,6-Dichloro resorcinol (**1**) (25.9 g, 145 mmol) and 4′-(8-octyloxy)-1,1′-biphenyl-4-carbonyl chloride (**2**) (5.00 g, 14.5 mmol) were dissolved in 250 mL anhydrous THF and 20 mL triethyl amine in a 500 mL round-bottom flask. The solution was stirred at 60 °C overnight and then quenched by cooling to room temperature and adding 50 mL 1 N HCl. The organic phase was washed with 10% KOH in water several times to remove the unreacted excess (**1**). The recovered organic phase was then washed with 1 N HCl three times and with a saturated solution of aqueous sodium bicarbonate before drying over MgSO$_4$. The desired product was isolated using column chromatography with 20% ethyl acetate in hexanes as the eluent to yield 6.0 g (12 mmol) (86% yield) of product. **^{1}H NMR:** δ 0.87–0.93 (t, 3H, –CH_3), δ 1.26–1.42 (m, 8H, –CH_2–), δ 1.46–1.52 (m, 2H, -OCH$_2$CH$_2$CH_2–), δ 1.78–1.88 (m, 2H, –OCH$_2$CH_2–), δ 4.00–4.60 (t, 2H, -OCH_2–), δ 5.62–5.66 (s, 1H, –OH), δ 7.04 (s, 1H, aromatic H on phenylene C ortho to aromatic COH), δ 7.00–7.04 (d, 2H, aromatic H on biphenyl ortho to –COC$_8$H$_{17}$), δ 7.48 (s, 1H, aromatic H on phenylene C ortho to aromatic CCl), δ 7.58–7.64 (d, 2H, aromatic H on biphenyl meta to –COC$_8$H$_{17}$), δ 7.70–7.74 (d, 2H, aromatic H on biphenyl meta to –COO–), δ 8.24–8.28 (d, 2H, aromatic H on biphenyl ortho to –COO–).

4,6-Dichloro-1-[4′-(8-octene-1-yloxy)-1,1′-biphenyl- 4 carboxylate]-3- [4′-(8-octyloxy)-1,1′-biphenyl- 4-carboxylate] phenylene (5)

Compounds (**3**) (6 g, 12.3 mmol) and (**4**) (4.2 g, 12.3 mmol) were dissolved in 100 mL anhydrous THF and 10 mL triethyl amine in a 500 mL round-bottom flask. The solution was stirred at 60 °C overnight, and the reaction was monitored by observing the emergence of an ^{1}H NMR peak at δ 7.58 and the disappearance of a peak at δ 7.48. After reacting for 20 h, the reaction was quenched by cooling to room temperature and adding 50 mL 1N HCl. The organic phase was washed with 1N HCl three times and then with a saturated solution of aqueous sodium bicarbonate. The organic phase was then collected and dried over MgSO$_4$, and the desired product was isolated using column chromatography with 5% ethyl acetate in hexanes as the eluent to yield 7.8 g (80% yield) of product. **^{1}H NMR:** δ 0.80–0.86 (t, 3H, –CH_3), δ 1.18–1.46 (m, 16H, –CH_2–), δ 1.70–1.80 (m, 4H, –OCH$_2$CH_2–), δ 1.98–2.02 (m, 2H, –CH_2CH$_2$=CH), δ 3.92–3.98 (t, 4H, –OCH_2–), δ 4.86–4.98 (q, 2H, –CH=CH_2), δ 5.70–5.80 (m, 1H, –CH=CH$_2$). δ 6.92–6.96 (d, 4H, aromatic H on biphenyl ortho to –COC$_8$H$_{17}$), δ 7.34 (s, 1H, aromatic H on phenylene C ortho to aromatic CCl), δ 7.50–7.56 (d, 4H, aromatic H on biphenyl meta to –COC$_8$H$_{17}$), δ 7.58 (s, 1H, aromatic H on phenylene C ortho to aromatic –COH), δ 7.62–7.66 (d, 4H, aromatic H on biphenyl meta to –COOAr), δ 8.18–8.20 (d, 2H, aromatic on biphenyl ortho to –COOAr) **^{13}C NMR:** δ 14.4 (-CH$_2$CH_3, 1C), δ 22.5 (-CH_2CH$_3$, 1C), δ 26–30 (Ar-OCH$_2$(CH_2)$_4$–, 8C), δ 32.0 (–CH_2CH=CH$_2$, 1C), δ 34.0 (–CH_2CH$_2$CH$_3$, 1C), δ 68.2 (Ar–OCH_2–, 2C), δ 114 (–CH=CH_2, 1C), δ 115.2 (aromatic C on

biphenyl ortho to –OCH_2–, 2C), δ 119.5 (aromatic C on phenylene meta to –Cl, 1C), δ 125.4 (aromatic C on biphenyl *C*–C═O, 2C), δ 126.4 (aromatic C on biphenyl ortho to –C═O, 2C), δ 127.0 (aromatic C on biphenyl meta to –$COCH_2$, 2C), δ 128.7 (aromatic *C*–Cl on phenylene, 2C), δ 131.0 (aromatic C on biphenyl para to –$COCH_2$, 2C), δ 131.3 (aromatic C on phenylene ortho to –CCl, 1C), δ 132.1 (aromatic C on biphenyl meta to –C═O, 2C), δ 140.0 (-*C*H═CH_2, 1C), δ 146.4 (aromatic *C*–O–C═O on phenylene, 2C), δ 146.8 (aromatic C on biphenyl para to –C═O, 2C), δ 159.9 (aromatic *C*–OCH_2 on biphenyl, 2C), δ 164.0 (*C*═O, 2C).

Preparation of bent core LCE. As shown in Scheme 2, elastomers were synthesized *via* a hydrosilylation reaction between Si–H groups of the polysiloxane polymer and terminal vinyl groups of the reactive bent-core mesogen (**5**) and the crosslinker 1,4-bis(11-undeceneoxy)benzene (**6**) (Scheme 2). In a typical procedure, the bent-core LC (**5**) (397 mg, 0.5 mmol), the crosslinker molecule (**6**) (24.8 mg, 0.06 mmol), and poly(hydrogen methylsiloxane) (36.0 mg, 0.58 mmol Si–H groups) were dissolved in a mixture of chloroform (0.3 mL) and thiophene-free toluene (1.1 mL). After all the components dissolved, 25 μL of a 1 wt% dichloro(1,5-cyclooctadiene)platinum(II) (Pt(COD)Cl_2) solution in methylene chloride was added. For all samples studied, the relative ratios of reagents was kept the same but the concentration of the reagents in the solvent was varied in some cases. The reaction solution was immediately loaded into a custom spin casting apparatus and spun for 6 h at 90 °C at 10,000 rpm. The spin casting head was then cooled to room temperature using dry ice, and the LCE film was carefully removed. At the end of the first stage of crosslinking, the elastomer was unaligned, lightly crosslinked, and swollen with toluene. Next, the LCE film was cut into strips approximately 3 cm in length and uniaxially deformed by loading the sample starting with a mass of 0.2 g and increasing the mass by 0.2 g every 60 min up to approximately 1 g. During the second step of crosslinking, the elastomer was initially isotropic due to solvent swelling but became nematic while heating and stretching. The swollen film turned hazy during the alignment process and then clear again as the polymer network aligned. After 20 h, the load was reduced to 0.4 g and the strips were placed in an oven at 50 °C for 48 h. The elastomer was then washed in an organic solvent to remove any residual, unreacted components. This was done by carefully immersing the LCE film in hexanes, followed by dropwise addition of toluene until the LCE enters the isotropic phase. Rapid addition of toluene may damage the LCE due to osmostic forces. After washing for several hours in toluene and hexanes, the elastomer film was dried under vacuum.

Instrumentation

X-Ray scattering. X-Ray scattering experiments were carried out on beamline X6B at the National Synchrotron Light Source at Brookhaven National Laboratory. Elastomer films of approximately 500 μm thickness were attached on one end to aluminium cassettes, across a 1.5 mm hole with ±15 degrees of angular range. The cassettes fit into a standard hot stage (Instec model HCS402) with a temperature stability of approximately 0.01 °C. The hot stage containing the sample cassette was mounted in a vacuum chamber and centered in an evacuated flight path on the beamline. The incident beam energy was 16 keV (wavelength 0.775 Å and energy resolution $\Delta E/E = 10^{-4}$); the beam cross-section was reduced to 0.2 mm horizontal × 0.3 mm vertical by slits placed 1 m upstream of the sample. Two dimensional SAXS images were recorded by a Princeton Instruments CCD area detector (2084 × 2084 array with 116 mm wide active area) located approximately 1.2 m from the sample. The correspondence between CCD pixel position on the detector and scattering wavenumber q was determined by calibration using a standard silver behenate powder placed at the sample position. The effective q resolution of the apparatus was 0.0033 $Å^{-1}$.

Differential scanning calorimetry. DSC measurements were performed with a TA Instruments Q200 DSC using heating and cooling rates of 5 °C per minute.

Polarized optical microscopy. The texture of the samples was observed using polarizing optical microscope Olympus BX60. The liquid crystal samples were placed in a computer-controlled hot stage (STC200F from INSTEC) that regulated the temperature with a precision better than 0.1 °C. The micrographs of the textures were captured using a Sony CCD camera. The transmitted light intensity was integrated over 1 mm^2 areas by a biased photodiode (U.O.T-455Hs from Oriel) in the eyepiece of the polarizing microscope. The light intensity was measured as a function of temperature using a Digital Multimeter (HP 34401A) and was used to identify the phase transitions.

Nuclear magnetic resonance. Solution ^1H and ^{13}C NMR spectroscopy were performed using a Varian VNMRS 500 MHz multinuclear spectrometer. Small molecule samples were placed in 5 mm o.d. tubes with sample concentrations of 1 and 5% (w/v) for ^1H and ^{13}C NMR, respectively. Chloroform-*d* (CDCl3) was used as the solvent, and residual solvent peaks serve as internal standards.

Thermoelastic measurements. The relative length $\lambda = L/L_0$ of the sample was determined as a function of temperature, where L is the length of the sample at a given temperature and L_0 is the length in the isotropic phase just above T_{NI}. The length was measured by placing fiduciary markers on the sample and recording the distance between the markers as a function of temperature under an applied load. A mass was attached to a 10 × 5 × 0.5 mm piece of BCE which was slowly heated in an oven. Temperature was monitored with a thermistor and a Velleman DVM345DI multimeter, and acrylic paint was used to make the marks along the length of the sample. A 35 mm digital camera was used to capture images of the BCE through the window of the oven to track the changes in distance between the marks.

Results and discussion

Synthesis and phase behavior of bent-core LC elastomers

Nematic BCEs were prepared by first synthesizing an asymmetric, reactive bent-core mesogen (**5**). The synthesis was accomplished by attaching each arm of the bent-core mesogen in separate steps (Scheme 1). The final reactive bent-core mesogen

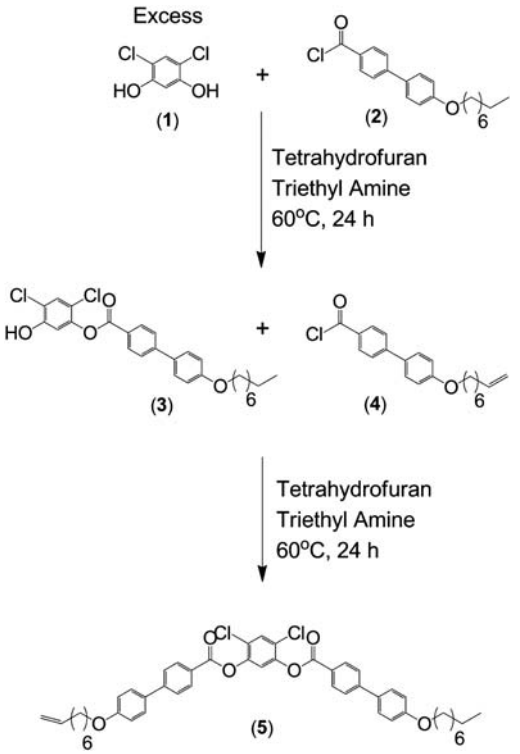

Scheme 1 Synthesis of reactive bent-core liquid crystal.

was isolated in an overall yield of 68%. This particular mesogen was chosen because it exhibits an enantiotropic nematic phase, in contrast to many other bent-core nematogens.[25] Interestingly, the functionalization of the alkyl tails with double bonds significantly influences the phase behavior of the LC, decreasing the T_{NI} by almost 10 °C relative to the bent-core LC without a terminal vinyl group.[24]

Uniformly aligned LC elastomers were prepared by using the reactive bent-core mesogenic monomers in a two-step crosslinking process (Scheme 2). In the first step, poly(hydrogen methylsiloxane) is simultaneously functionalized by (**5**) and crosslinked by (**6**) *via* hydrosilylation reactions catalyzed by a Pt catalyst. This first step is carried out in toluene and chloroform and gives a lightly crosslinked (but unaligned) LC elastomer. In the second step, the elastomer is stretched and heated to uniformly align the mesogens in the direction of stretching. This second step aligns and further crosslinks the elastomer to lock in the orientation defined by stretching. After these two steps, the elastomer is washed with a mixture of hexanes and toluene to remove any unreacted material.

This method has been widely used to produce a variety of LC elastomers with calamitic LC side-groups but never before with bent-core mesogenic side groups. The method can successfully produce BCEs (Fig. 2), but achieving well-aligned, optically clear samples is challenging. The preparation method was systematically varied to undertsand the relative importance of various reaction parameters on the optical quality of the LCEs (Table 1). We investigated the effect of the temperature during crosslinking, the concentration of the reagents during crosslinking, and the effect of washing the elastomer with toluene. The concentration of the reactive bent-core monomer was the most important factor for achieving optically clear samples (Fig. 2). The clearest and most uniform films were obtained by using a more dilute concentration of reagents (0.25 mM of bent-core compared with 0.5 mM). Samples with high concentrations of the initial reactants were dark in color. Polarized optical microscopy reveals that all BCEs were aligned, and the sample with the best optical clarity, BCE3, also has the highest uniformity (Fig. 2). The lower optical quality and poorer alignment of samples with higher concentration may be due to the limited solubility of (**5**) in toluene, which can result in a higher concentration of unreacted mesogen in the final elastomer sample. However, washing the dark elastomers with hexanes and toluene did little to improve the optical clarity and color of the darker films, which was also true for varying the temperature and reaction time.

The phase behavior of the reactive bent-core LC (**5**) and the bent-core elastomers is given in Table 1. The BCEs are glassy solids at room temperature and exhibit nematic phases just above room temperature while the reactive bent-core LC is crystalline at room temperature and exhibits a nematic phase at much higher temperatures. The latent heats measured for the nematic-to-isotropic transitions in the BCEs are similar to those for other nematic LCEs.[22] Despite the clear differences in the texture, clarity, and quality of alignment, all four BCEs display similar

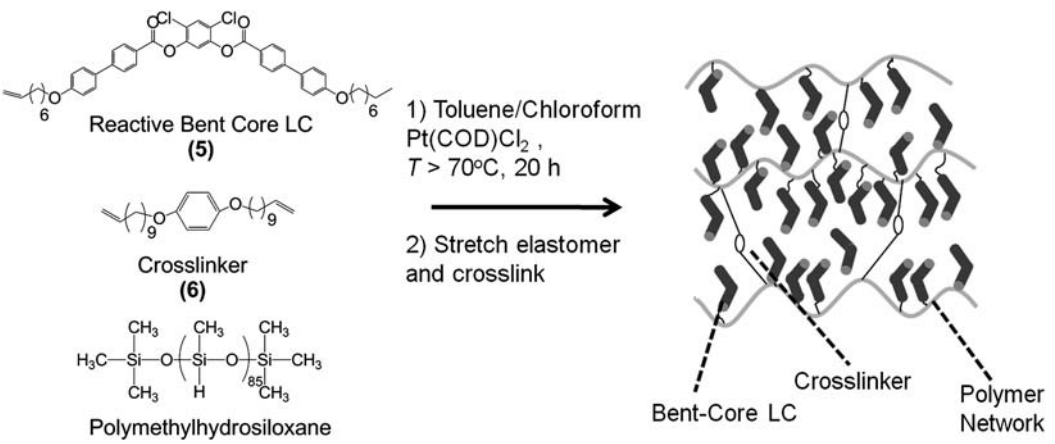

Scheme 2 Synthesis of aligned bent-core liquid crystal elastomer (BCE).

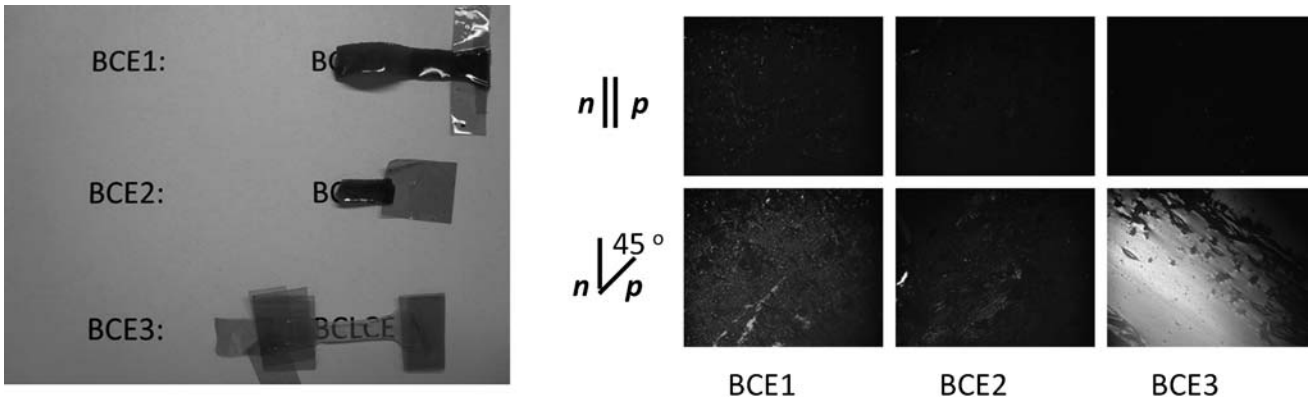

Fig. 2 A photograph of the bent-core elastomers produced in this study (left) and polarizing optical micrographs of BCE 1–3 (right). BCE3 exhibits the best optical clarity. BCE4 is not shown but has optical quality comparable to BCE1 and BCE2. The polarizing optical microscopy frames show that BCE3 also has the highest birefringence, indicating better alignment of the LC side groups.

Table 1 Reaction conditions and properties of bent-core elastomers (BCEs) and the reactive bent-core LC (BCLC) (**5**)

sample	Reaction Temp. (°C)[a]	Monomer Concentration (mM)[b]	Toluene Wash[c]	Soluble Fraction	T_{NI} [d] (°C)	$\Delta H_{N\,I}$ (J g^{-1})	T_g or T_m [e] (°C)
BCLC (**5**)	N/A	N/A	N/A	N/A	108.1	1.987	47.9
BCE1	90	0.5	No	19.1%	109.7	0.957	23.9
BCE2	90	0.5	Yes	20.2%	109.5	1.110	32.9
BCE3	90	0.25	Yes	17.8%	108.7	0.752	26.0
BCE4	70	0.5	Yes	20.0%	107.0	0.877	30.0

[a] Temperature at which the crosslinking reaction is carried out. [b] Concentration of monomer in crosslinking reaction. The concentrations of all other reagents are scaled to keep the relative reagent concentrations the same in all cases. [c] Samples were immersed in a mixture of hexanes and toluene to remove unreacted LC mesogen. BCE1 was not washed before analyzing by polarizing optical microscopy and observing the optical quality as in Fig. 2, but all samples were washed before measurement by DSC. [d] T_{NI} identified by the onset of the phase transition *via* DSC during heating. [e] All BCEs exhibit a glass transition temperature (T_g) while the reactive bent-core LC (**5**) shows a crystallization/melting transition at temperature T_m.

phase behavior. Therefore, while alignment and optical clarity depend sensitively on the preparation details examined, the thermal properties are relatively insensitive to these details. Notably, while bent-core LCs are typically crystalline near room temperature, BCEs have a nematic phase at temperatures as low as 30 °C, enabling applications of nematic bent-core LCs that require near-room temperature operation.

Thermoelastic behavior

A distinguishing characteristic of aligned LC elastomers is their ability to reversibly change shape with temperature.[6,7] This effect is due to the temperature-dependent conformation of the polymers in the elastomeric network which is strongly coupled to the liquid crystal order parameter. Due to the limitation of material and the possibility for sample rupture during measurement, the thermoelastic properties of only the best sample, BCE3, were investigated in detail. However, the phase behavior presented in the previous section and the SAXS results in the subsequent section indicate that the structure of all the BCE samples produced is qualitatively similar despite differences in the optical qualities. Therefore, we expect the thermoelastic behavior of all of the BCE samples studied to be qualitatively similar.

BCE3 shows reversible thermoelastic behavior (Fig. 3). As expected, with increasing temperature the elastomer decreases in length due to a decreasing LC order parameter. The sample shrinks in the direction parallel to the nematic director. On cooling the sample from temperatures above T_{NI} to room temperature, the sample spontaneously expands to more than twice its initial length; this response is fully reversible on heating. The magnitude of this relative change in shape is commensurate with that typically seen in calamitic side-chain LCEs[22] and greater than that observed for nematic LCEs swollen with small molecule bent-core LCs[24] as well as for smectic LCEs.[26]

These thermoelastic measurements indicate that, despite the much larger bent-core mesogen, the elastic properties of BCEs are similar to those of calamitic LCEs. Spontaneous shape deformations follow the predictions of a Landau-de Gennes model for the LC order along with additional terms for rubber elasticity.[7,22] With respect to sample texture, optical clarity,

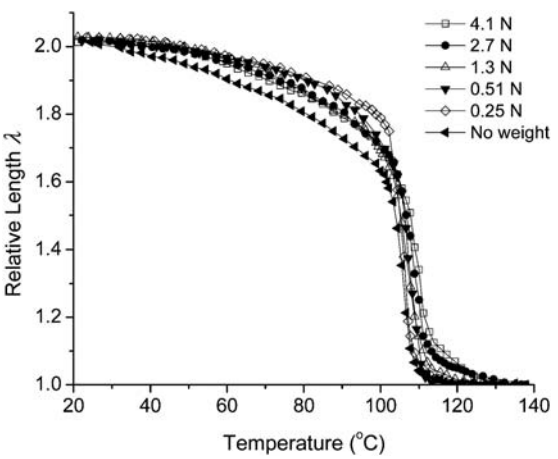

Fig. 3 Thermoelastic behavior of sample BCE3 under different loads. The relative length λ is given by the ratio of the length of the sample at a given temperature to the sample length just above T_{NI}. A force of 0.25 N corresponds to a stress of 0.98 kPa.

modulus, and thermoreversible elasticity, BCEs are indistinguishable from the well-studied calamitic side-chain LCEs.

X-Ray scattering studies

Small-angle X-ray scattering (SAXS) studies were carried out to investigate positional and orientational order present in the BCEs. Several recent reports on nematic bent-core LCs[12,16,19,20,27,28] found that nematic bent-core LCs exhibit small-angle scattering patterns inconsistent with a uniaxial nematic phase. Specifically, uniaxial nematics only have long-range orientational order and are expected to show two broad wide-angle peaks (corresponding to short-range positional correlations along the short-axis of the molecules) and two broad low-angles peaks (corresponding to short-range positional correlations along the long-axis of the molecules). By contrast, smectics and higher order LCs exhibit sharp peaks that reflect long-range positional ordering.[29] Near a nematic-to-smectic transition, nematics can exhibit short-range smectic ordering reflected by an increased intensity and decreased width of the low-angle peaks and, in the case of a smectic C phase at lower temperature, an additional splitting of the peaks due to an azimuthal degeneracy of the local layer orientation when the tilted director is aligned.[30,31] The peaks remain broad and diffuse because the smectic correlations are only short-ranged. On the other hand, bent-core nematics show multiple low-angle peaks over a broad temperature range,[27,28,32] even when no underlying smectic phase is present.[19,20] Here, we are interested in investigating the SAXS pattern of BCEs to understand their structure and relationship to previous studies of nematic bent-core LCs.

SAXS measurements of BCE samples were carried out over a q-range of approximately 0.1 $Å^{-1}$ to 1 $Å^{-1}$, well-suited to studying the lengthwise positional correlations of the bent-core molecules (with an approximate length of 45 Å). The SAXS patterns of all BCEs show four distinct low-angle maxima in diffracted intensity at all temperatures studied (Fig. 4). For each sample, the pattern is anisotropic even at temperatures above T_{NI}. The orientational ordering of the mesogens during cross-linking is permanently imprinted in the BCEs. Furthermore, the peaks are more diffuse at higher temperatures, indicating more disorder (Fig. 4). Upon cooling below T_{NI}, the anisotropy and sharpness of the peaks increase, as expected for an increasing nematic order parameter. This is clearly revealed in Fig. 4b, which is obtained for BCE4 by averaging the data over a rectangular region as indicated in the figure. As the temperature is decreased from T_{NI} to temperatures well below T_{NI}, the peaks sharpen and move from 38° to 45° relative to the preferred direction.

A comparison of pure bent-core LCs and BCEs reveals important differences between the elastomeric and small molecule materials (Fig. 4 and Fig. 6). First, while the bent-core LCs are isotropic at temperatures above the T_{NI}, the BCEs remain anisotropic at all temperatures. This is observed in most nematic LCEs.[7] Second, the separation of the low-angle peak is more distinct in BCEs, while there is considerable overlap between the low-angle peaks in the pure bent-core LCs even at temperatures below (but close to) T_{NI}.

The presence of a fourfold pattern of broad, low-angle peaks indicates short-range positional correlations inconsistent with the uniaxial symmetry of the nematic phase. Two explanations for the smectic-like low-angle peaks in bent-core LCs have been proposed. The first is that the intrinsic bent shape of the molecules can give rise to splitting in the low-angle peaks and the angular position of the low-angle peaks is related to the angle

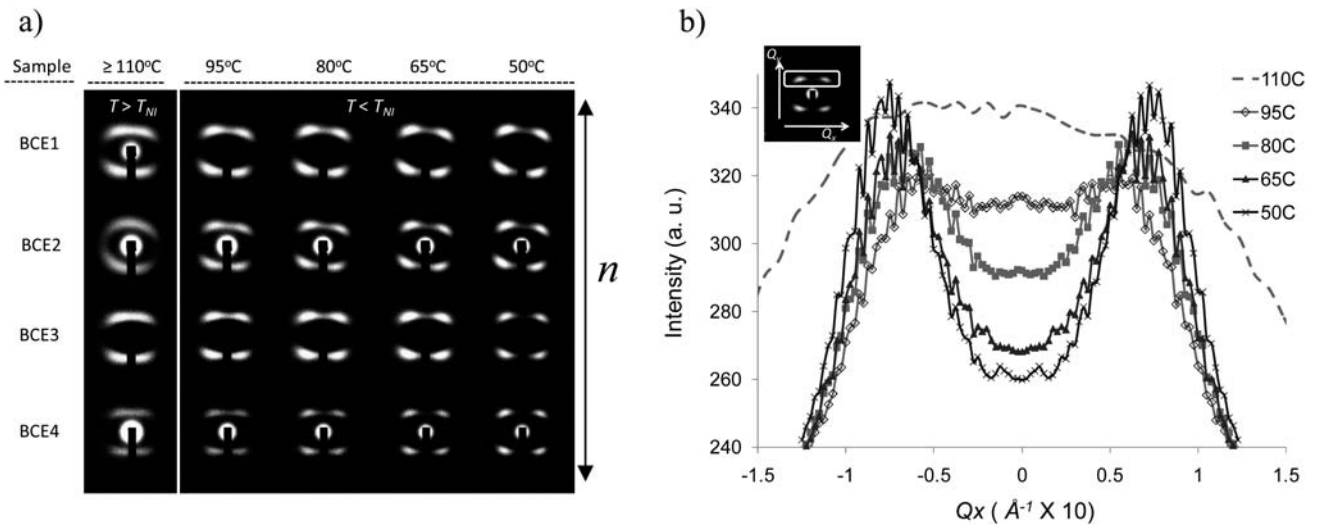

Fig. 4 (**a**) SAXS patterns for BCEs as a function of temperature and (**b**) temperature dependent scattering profile for BCE4 averaged over a rectangular section. **4a**: The preferred alignment direction is indicated by the double arrow. The highest temperature shown for BCE1, BCE2, and BCE3 is 115 °C and 110 °C for BCE4. All samples display qualitatively similar behavior, indicating anisotropy in the scattering pattern at all temperatures, even in the isotropic phase. In the nematic phase, the samples exhibit four distinct low-angle scattering peaks. Some details vary from sample to sample, such as the diffuse scattering around the beam stop (stronger for thicker elastomers) and the position of the four peaks. The tilt angle in some of the patterns reflects a slight tilt in the sample during measurement. **4b**: The data for BCE4 are averaged over the rectangular region shown. As the temperature decreases from 110 °C to 50 °C, the intensity maxima moves to larger angles relative to the nematic director. The angle changes from 38° to 45° at low temperatures.

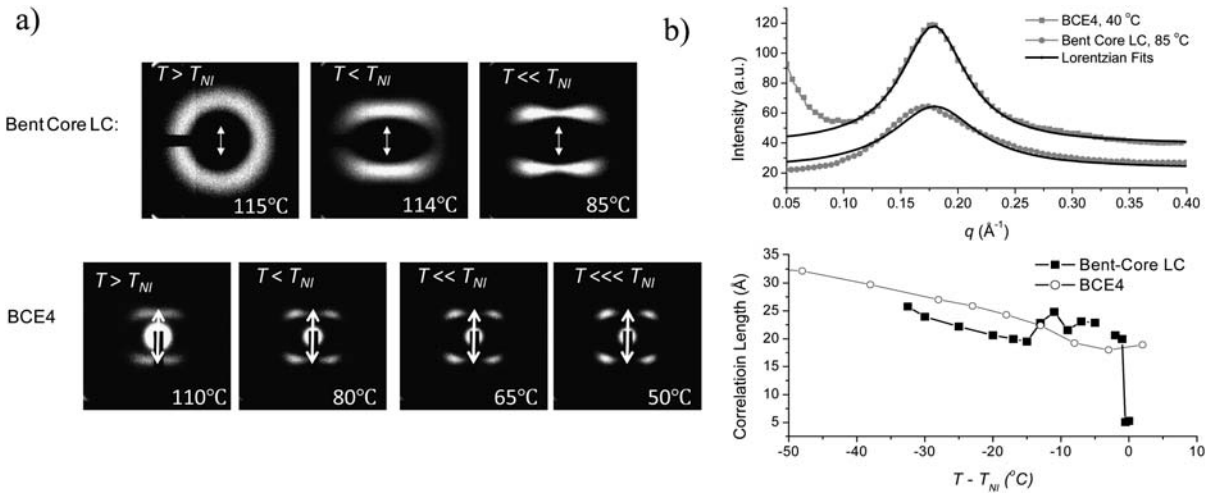

Fig. 5 (a) Temperature dependent scattering profiles for a bent-core LC (under magnetic field alignment) and BCE4 and (**b**) Lorentzian model fitting to the scattered intensity for BCE4 along with correlation lengths derived from model fitting. The bent-core LC is identical to (**5**) but without the terminal vinyl group, and the T_{NI} of the bent-core LC is 115 °C[24]. The scatter in the correlation length for the bent-core LC is due to greater uncertainty in the position of the maximum.

between the two arms of the bent-core molecules (~140°).[12] A second explanation is that, as in certain calamitic nematics, nematic bent-core LCs exhibit short-range smectic C-type ordering.[16,18–20,28,33–34] By the latter hypothesis, the splitting of the low-angle peaks reflects the tilt angle of the molecules relative to the direction normal to the smectic layer spacing. The hypothesis of short-range smectic C order or "clusters" provides a straightforward explanation for the temperature dependent shift in the peak positions to higher q as noted above (and shown in Fig. 4) – namely, that the tilt angle (and consequently layer spacing) increases slightly with decreasing temperature.

The phenomenological description of short-range smectic order presented in ref. 19 provides a basis to estimate the smectic cluster correlation length from the broadness of the diffraction peaks. This approach is typically used to describe smectic ordering in the vicinity of a nematic-to-smectic transition, and it reasonably accounts for the basic features of the SAXS data recorded over the full nematic range of the bent-core mesogen on which the bent-core monomer in Scheme 1 is based. The theory predicts a Lorentzian distribution of scattered intensity, from which a cluster "size" (or distance over which smectic ordering persists) can be extracted from the peak widths (full-width at half maximum is the inverse of the smectic correlation length). This type of analysis shows that the cluster size in both bent-core LCs and BCEs are similar and exhibit similar temperature dependencies, except upon crossing the T_{NI} where the correlation length for bent-core LCs drops to a value that corresponds approximately to the width (~5 Å) of the molecules (Fig. 5).

Conclusions

Uniformly aligned BCEs were prepared using a two-step cross-linking method with a reactive bent-core mesogen and a polysiloxane polymer. The resulting BCEs are optically clear under certain preparation conditions, and phase behavior studies reveal a nematic phase at temperatures near room temperature. The thermoelastic behavior of BCEs is similar to that of calamitic LCEs, with reversible elongation of more than 100%. SAXS measurements show multiple, low-angle scattering peaks similar to those seen in calamitic nematics in the vicinity of a nematic-to-smectic C phase transition. The general features of the low-angle scattering patterns of BCEs are qualitatively similar to those of pure bent-core LCs. In both cases, a pattern inconsistent with uniaxial nematic symmetry, but consistent with short-range smectic C order, emerges. The typical size of the smectic clusters is similar for the BCEs and the pure bent-core LC on which they are based. Flexoelectric measurements on the materials reported here[21] confirm that BCEs exhibit an enhanced flexoelectric response, similar to that for pure bent-core LCs. This study and these recent measurements suggest that BCEs are promising materials for advanced applications that take advantage of the unique properties of bent-core LCs.

Acknowledgements

We are indebted to Ron Pindak for several helpful conversations. This work at Kent State University was supported by NSF Grant No. DMR-0606160 and Office of Naval Research Grant No. N00014-07. A portion of this research was conducted at the Center for Nanophase Materials Sciences, which is sponsored at Oak Ridge National Laboratory by the Division of Scientific User Facilities, U.S. Department of Energy. Use of the National Synchrotron Light Source, Brookhaven National Laboratory, was supported by the U.S. Department of Energy, Office of Science, Office of Basic Energy Sciences, under Contract No. DE-AC02-98CH10886. The elastomers were prepared by the New Liquid Crystal Materials Facility at Kent State University, a program sponsored by the NSF Grant No. DMR-0606357, the Ohio Department of Development, and Alpha Micron, Inc.

Notes and references

1 H. Finkelmann, E. Nishikawa, G. G. Pereira and M. Warner, *Phys. Rev. Lett.*, 2001, **87**, 015501.

2 M. Yamada, M. Kondo, R. Miyasato, Y. Naka, J.-i. Mamiya, M. Kinoshita, A. Shishido, Y. Yu, C. J. Barrett and T. Ikeda, *J. Mater. Chem.*, 2009, **19**, 60–62.
3 Y. Hong, B. Axel, J.-M. Taulemesse, K. Kaneko, S. Mery, A. Bergeret and P. Keller, *J. Am. Chem. Soc.*, 2009, **41**, 15000–15004.
4 M. D. Kempe, N. R. Scruggs, R. Verduzco, J. Lal and J. A. Kornfield, *Nat. Mater.*, 2004, **3**, 177.
5 S. Krause, F. Zander, G. Bergmann, H. Brandt, H. Wertmer and H. Finkelmann, *C.R. Chimie*, 2009, **12**, 85–104.
6 K. Urayama, *Macromolecules*, 2007, **40**, 2277–2288.
7 M. Warner and E. M. Terentjev, *Liquid Crystal Elastomers*, Oxford University Press, Oxford, 2003.
8 J. Küpfer and H. Finkelmann, *Macromol. Chem., Rapid Commun.*, 1991, **12**.
9 M. Blanca Ros, J. L. Serrano, M. Rosario de la Fuente and C. L. Folcia, *J. Mater. Chem.*, 2005, **15**, 5093–5098.
10 D. M. Walba, E. Körblova, R. Shao, J. E. Maclennan, L. D. R., M. A. Glaser and N. A. Clark, *Science*, 2000, **288**, 2181–2184.
11 H. Takezoe and Y. Takanishi, *Jpn. J. Appl. Phys.*, 2006, **45**, 597–625.
12 B. R. Acharya, A. Primak and S. Kumar, *Phys. Rev. Lett.*, 2004, **92**, 145506.
13 L. A. Madsen, T. J. Dingemans, M. Nakata and E. T. Samulski, *Phys. Rev. Lett.*, 2004, **92**, 145505.
14 J. Harden, B. Mbanga, N. Éber, K. Fodor-Csorba, S. Sprunt, J. T. Gleeson and A. Jákli, *Phys. Rev. Lett.*, 2006, **97**, 157802.
15 C. Bailey, K. Fodor-Csorba, S. Sprunt, J. T. Gleeson and A. Jákli, *Phys. Rev. Lett.*, 2009, **103**, 237803.
16 V. Görtz, C. Southern, N. W. Roberts, H. F. Gleeson and J. W. Goodby, *Soft Matter*, 2009, **5**, 463–471.
17 C. Bailey and A. Jákli, *Phys. Rev. Lett.*, 2007, **99**.
18 S. Stojadinovic, A. Adorjan, S. Sprunt, H. Sawade and A. Jakli, *Phys. Rev. E: Stat., Nonlinear, Soft Matter Phys.*, 2002, **66**, 060701.
19 S. H. Hong, R. Verduzco, J. Williams, R. J. Twieg, E. Dimasi, R. Pindak, A. Jákli, J. T. Gleeson and S. Sprunt, *Soft Matter*, 2010, DOI: 10.1039/c000362j.
20 C. Keith, A. Lehmann, U. Baumeister, M. Prehm and C. Tschierske, *Soft Matter*, 2010, **6**, 1704–1721.
21 J. Harden, M. Chambers, R. Verduzco, P. Luchette, J. T. Gleeson, S. Sprunt and A. Jakli, *Appl. Phys. Lett.*, 2010, **96**, 102907.
22 H. Finkelmann, A. Greve and M. Warner, *Eur. Phys. J. E*, 2001, **5**, 281–293.
23 K. Fodor-Csorba, A. Jákli and G. Galli, *Macromol. Symp.*, 2004, **218**, 81–88.
24 M. Chambers, R. Verduzco, J. T. Gleeson, S. Sprunt and A. Jákli, *Adv. Mater.*, 2009, **21**, 1622.
25 K. Fodor-Csorba, A. Vajda, A. Jákli, C. Slugovc, G. Trimmel, D. Demus, E. Gács-Baitz, S. Holly and G. Galli, *J. Mater. Chem.*, 2004, **14**, 2499–2506.
26 A. Komp and H. Finkelmann, *Macromol. Rapid Commun.*, 2007, **28**, 55–62.
27 C. Southern, P. D. Brimicombe, S. D. Siemianowski, S. Jaradat, N. Roberts, V. Görtz, J. W. Goodby and H. F. Gleeson, *Europhys. Lett.*, 2008, **82**, 56001.
28 N. Vaupotič, J. Szydlowska, M. Salamonxzyk, A. Kovarova, J. Scoboda, M. Osipov, D. Pociecha and E. Gorecka, *Phys. Rev. E: Stat., Nonlinear, Soft Matter Phys.*, 2009, **80**, 030701.
29 S. Kumar, in *Liquid Crystals*, ed. S. Kumar, Cambridge University Press, Cambridge, 2001, pp. 65–94.
30 W. L. McMillan, *Phys. Rev. A: At., Mol., Opt. Phys.*, 1973, **7**, 1673–1678.
31 W. L. McMillan, *Phys. Rev. A: At., Mol., Opt. Phys.*, 1973, **8**, 328–331.
32 V. Prasad, S.-W. Kang, K. A. Suresh, L. Joshi, Q. Wang and S. Kumar, *J. Am. Chem. Soc.*, 2005, **127**, 17224–17227.
33 V. Domenici, C. A. Veracini and B. Zalar, *Soft Matter*, 2005, **1**, 408.
34 G. Cinacchi and V. Domenici, *Phys. Rev. E: Stat., Nonlinear, Soft Matter Phys.*, 2006, **74**, 030701.